Electronic Supplementary Material (ESI) for Green Chemistry.

Supplementary Information

Structure Sensitivity of the Electrochemical Hydrogenation of *cis,cis*-Muconic Acid to Hexenedioic Acid and Adipic Acid

Deep M. Patel,[a,b,‡] Prathamesh T. Prabhu,[a,b,‡] Geet Gupta,[a,b] Marco Nazareno Dell'Anna,[a,b] Samantha Kling,[a,b] Huy T. Nguyen,[a,b] Jean-Philippe Tessonnier,*[a,b] and Luke T. Roling*[a,b]

[a] Department of Chemical and Biological Engineering, Iowa State University, Ames, IA 50011, USA.

[b] Center for Biorenewable Chemicals (CBiRC), Ames, IA 50011, USA.

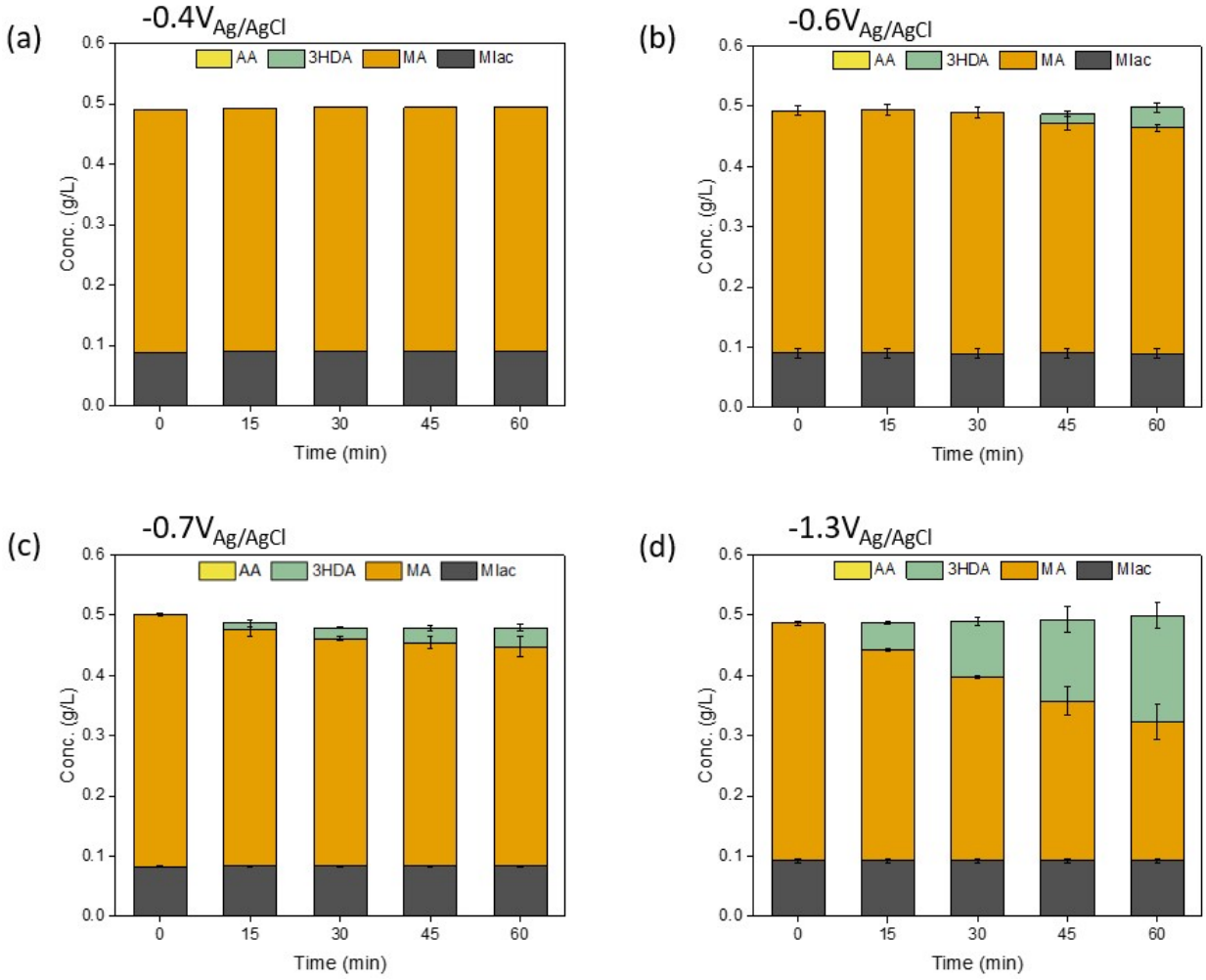

Fig. S1 Concentration (g/L) of reactants and products in solution during chronoamperometry (CA) experiments performed for 1 hour on Pt foil at respective potentials. The error bars represent standard error from triplicates. Notation: muconic acid (MA), *trans*-3-hexenedioic acid (3HDA), muconolactone (Mlac).

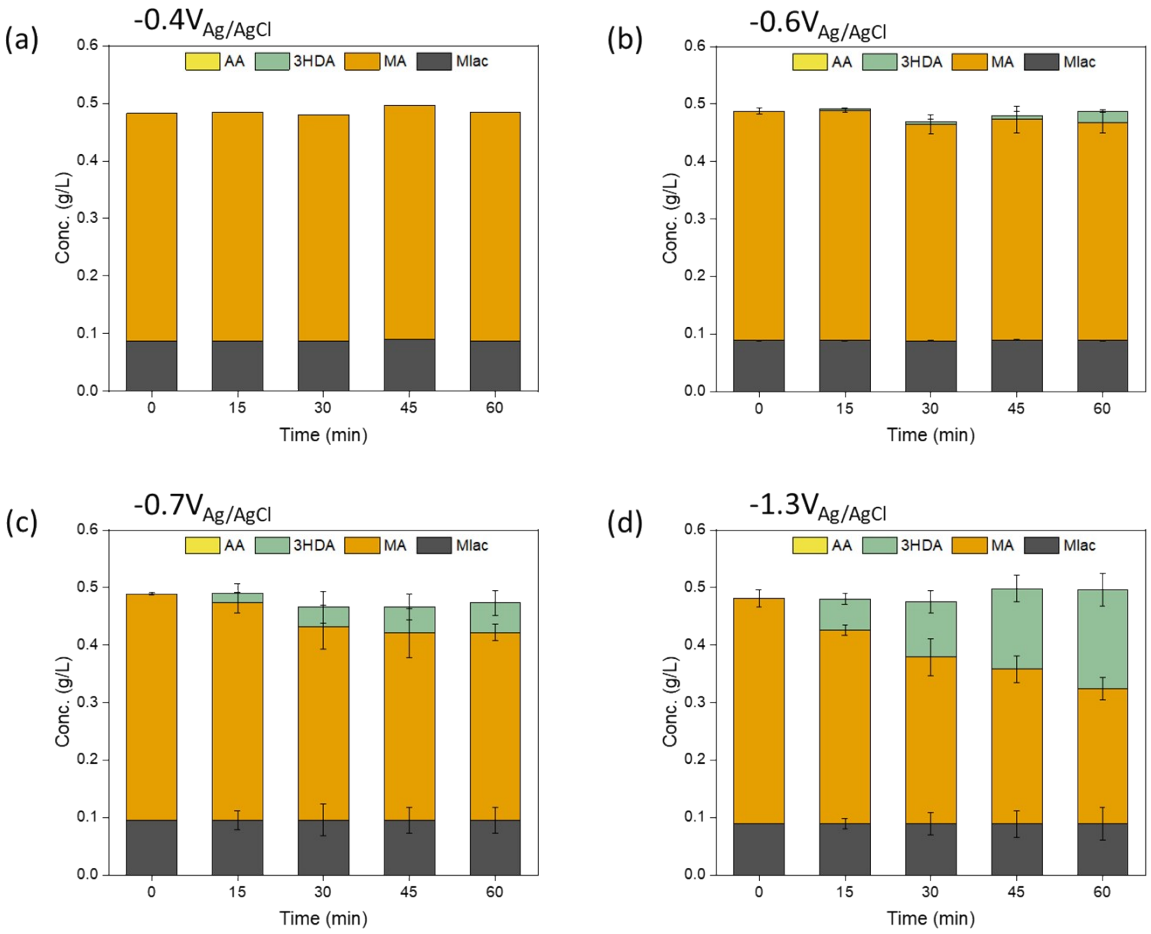

Fig. S2 Concentration (g/L) of reactants and products in solution during chronoamperometry (CA) experiments performed for 1 hour on Pd foil at respective potentials. The error bars represent standard error from triplicates. Notation: *cis,cis*-muconic acid (*cc*MA), *trans*-3-hexenedioic acid (3HDA), muconolactone (Mlac).

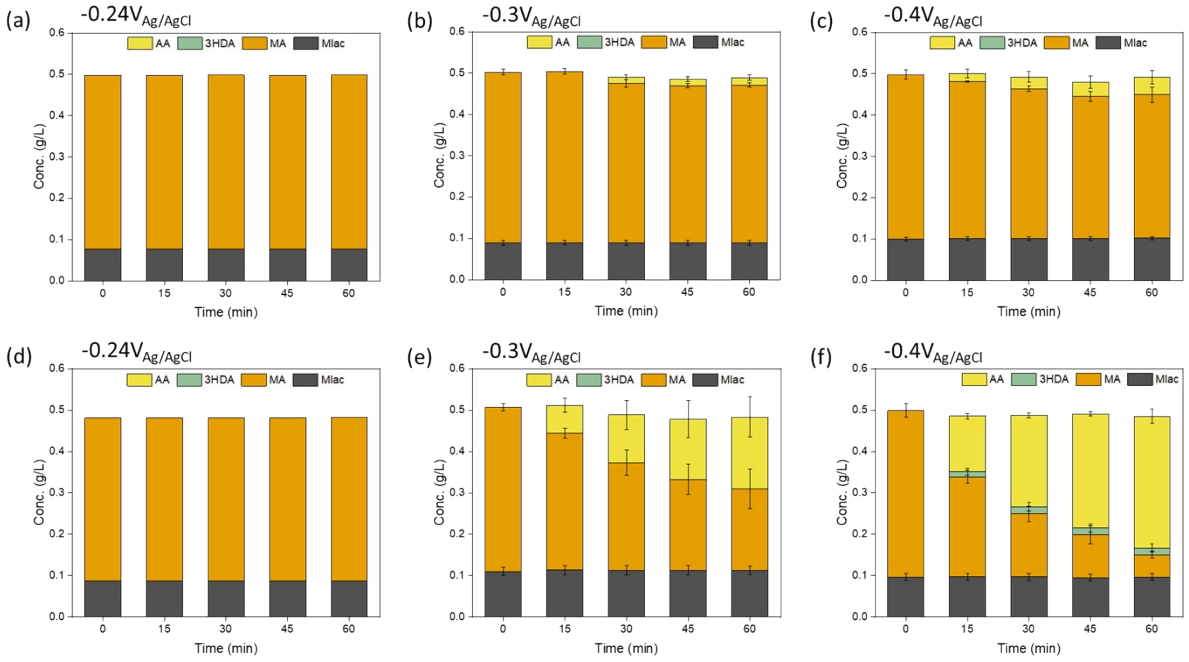

Fig. S3 Concentration (g/L) of reactants and products in solution during chronoamperometry (CA) experiments performed for 1 hour at respective potentials on 1 mg of (a)-(c) Pt/C, and (d)-(f) Pd/C. The error bars represent standard error from triplicates. Notation: muconic acid (MA), *trans*-3-hexenedioic acid (3HDA), adipic acid (AA), muconolactone (Mlac).

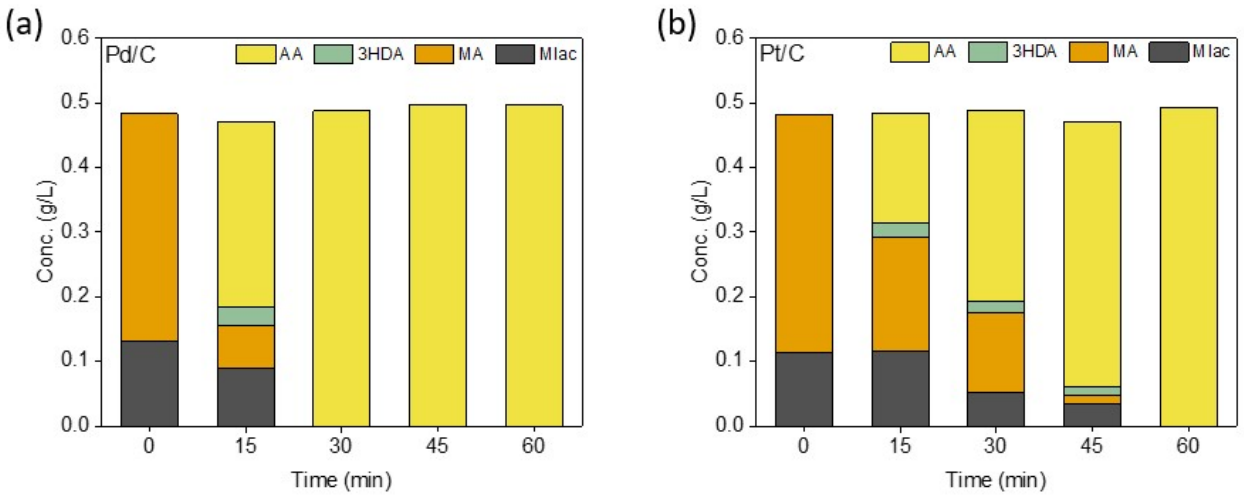

Fig. S4 Concentration (g/L) of reactants and products in solution during chronoamperometry (CA) experiments performed for 1 hour at -0.4 $V_{Ag/AgCl}$ on 10 mg of (a) Pd/C, and (b) Pt/C. Notation: muconic acid (MA), *trans*-3-hexenedioic acid (3HDA), muconolactone (Mlac), and adipic acid (AA).

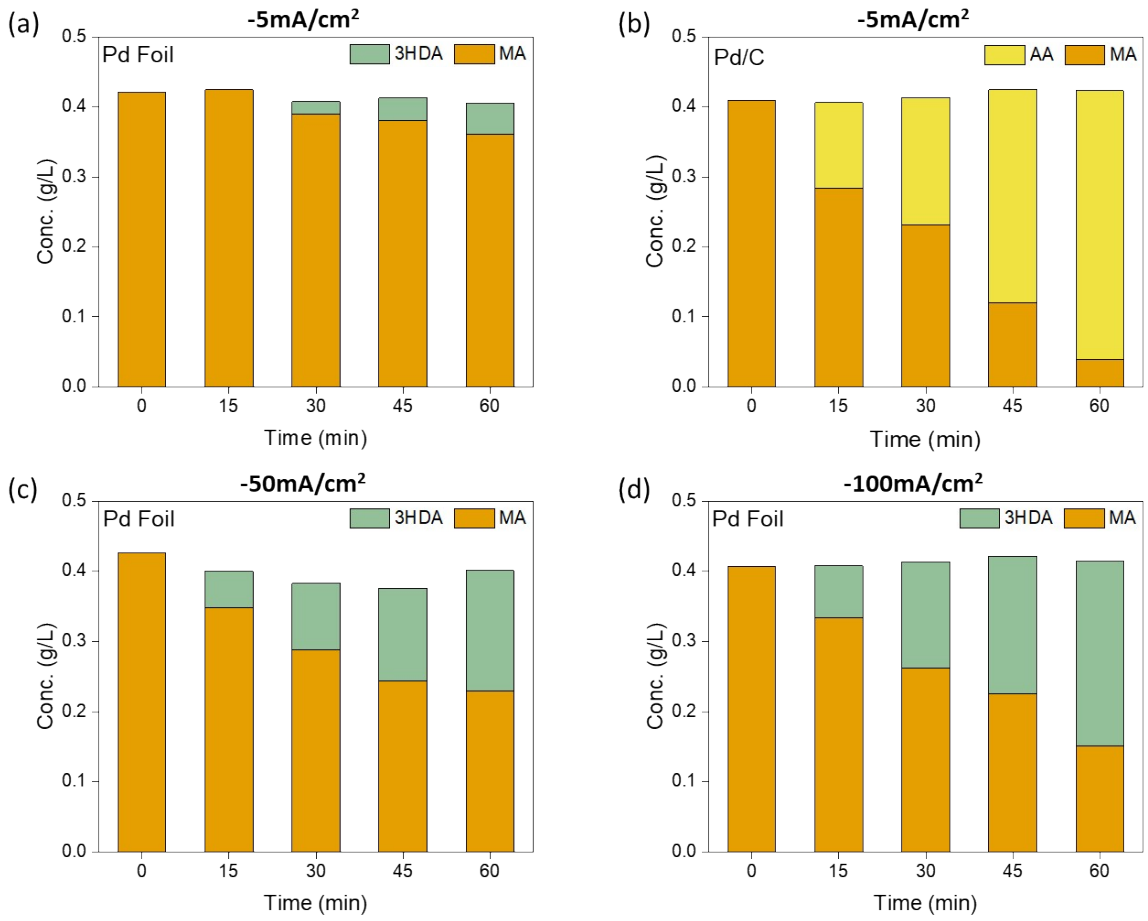

Fig. S5 Concentration (g/L) of reactants and products in solution during chronopotentiometry (CP) experiments performed for 1 hour at respective current densities on (a),(c),(d) Pd foil, and (b) Pd/C. Notation: muconic acid (MA), *trans*-3-hexenedioic acid (3HDA), and adipic acid (AA).

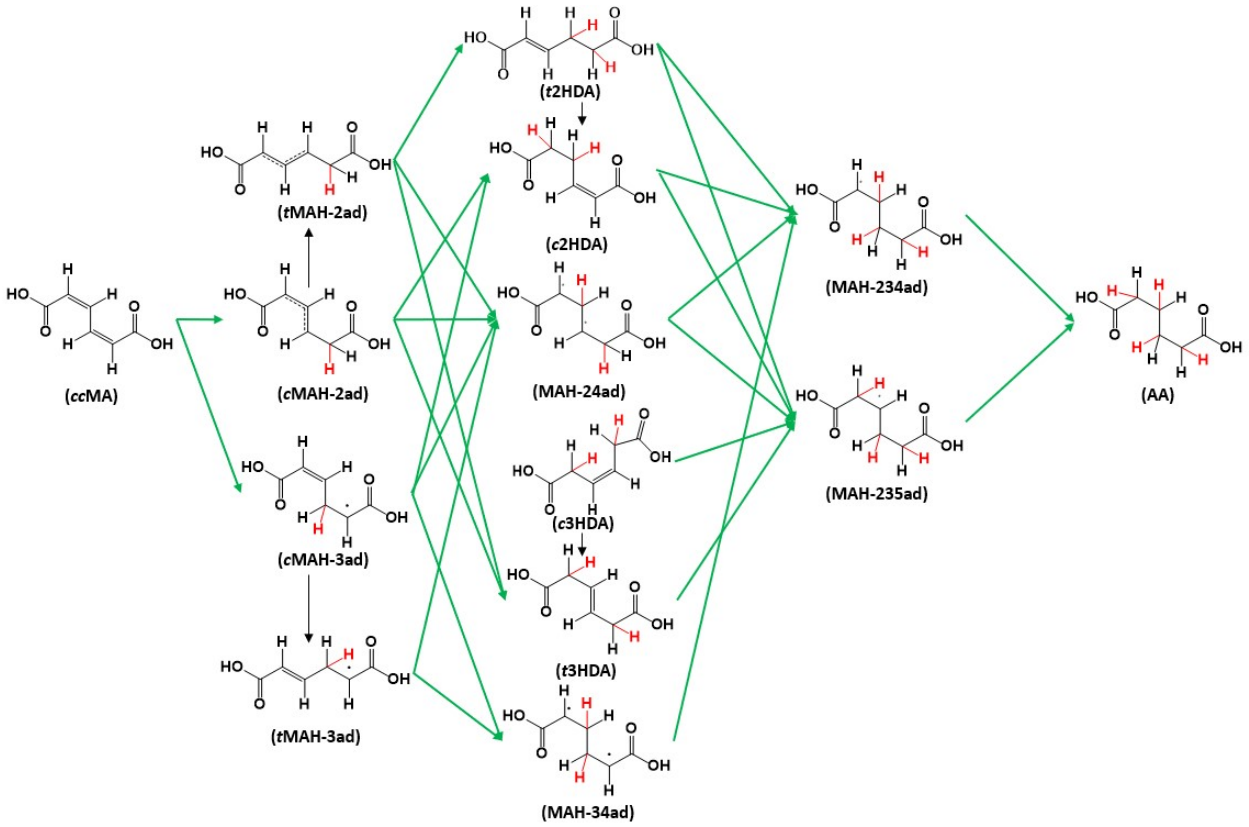

Fig. S6 Reaction network showing all the elementary steps considered for electrochemical hydrogenation of *cis,cis*-muconic acid (*cc*MA) to *trans*-2-hexenedioic acid (*t*2HDA), *trans*-3-hexenedioic acid (*t*3HDA), and adipic acid (AA) on (111) and (533) surfaces of Pd and Pt, and in solution. Green arrows denote electrochemical steps and black arrows denote non-electrochemical steps.

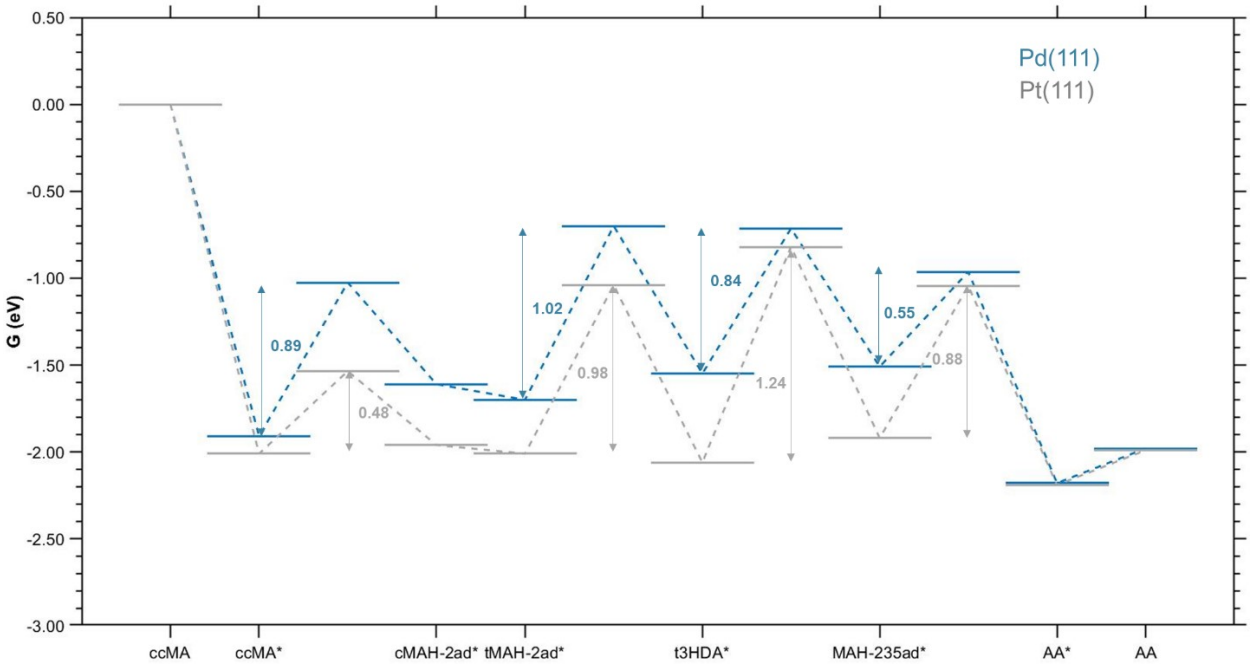

Fig. S7 Free energy (G, eV) diagram for the *cc*MA* → *t*3HDA* → AA* pathway on Pd(111) and Pt(111) surfaces at 0.00 V_{RHE}, pH 0, and 298 K. Notation: *cis,cis*-muconic acid (*cc*MA), *trans*-3-hexenedioic acid (*t*3HDA), adipic acid (AA). Here, "*" denotes adsorbed species.

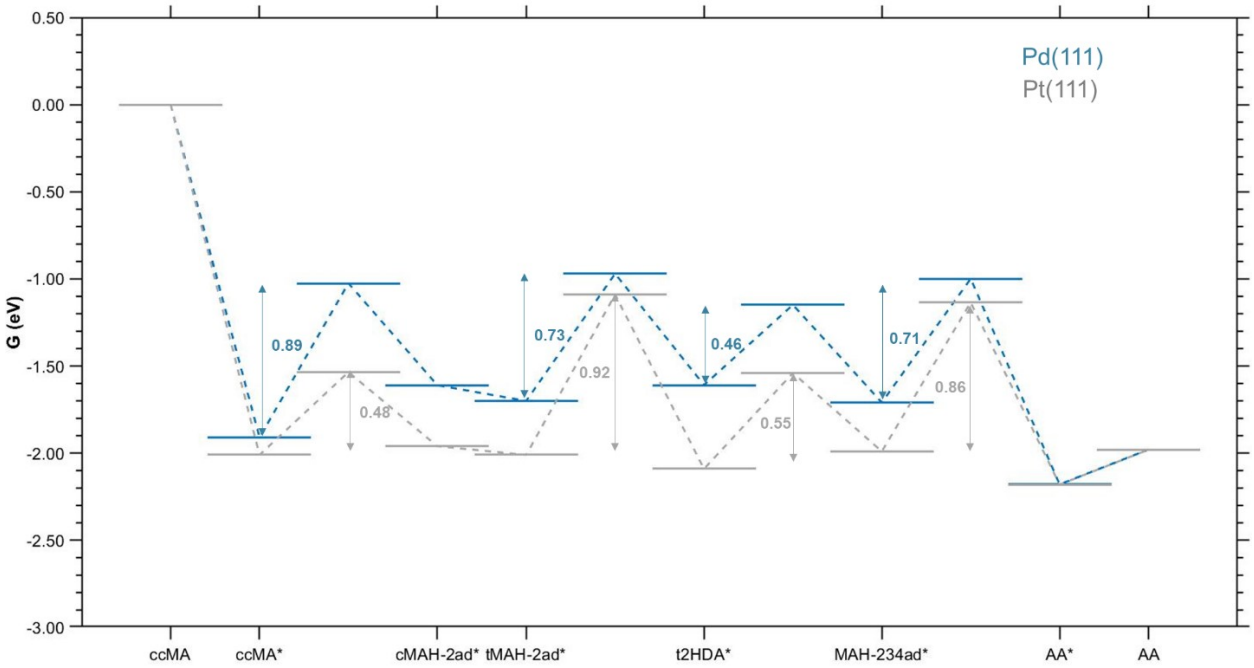

Fig. S8 Free energy (G, eV) diagram for the *cc*MA* → *t*2HDA* → AA* pathway on Pd(111) and Pt(111) surfaces at 0.00 V_{RHE}, pH 0, and 298 K. Notation: *cis,cis*-muconic acid (*cc*MA), *trans*-2-hexenedioic acid (*t*2HDA), adipic acid (AA). Here, "*" denotes adsorbed species.

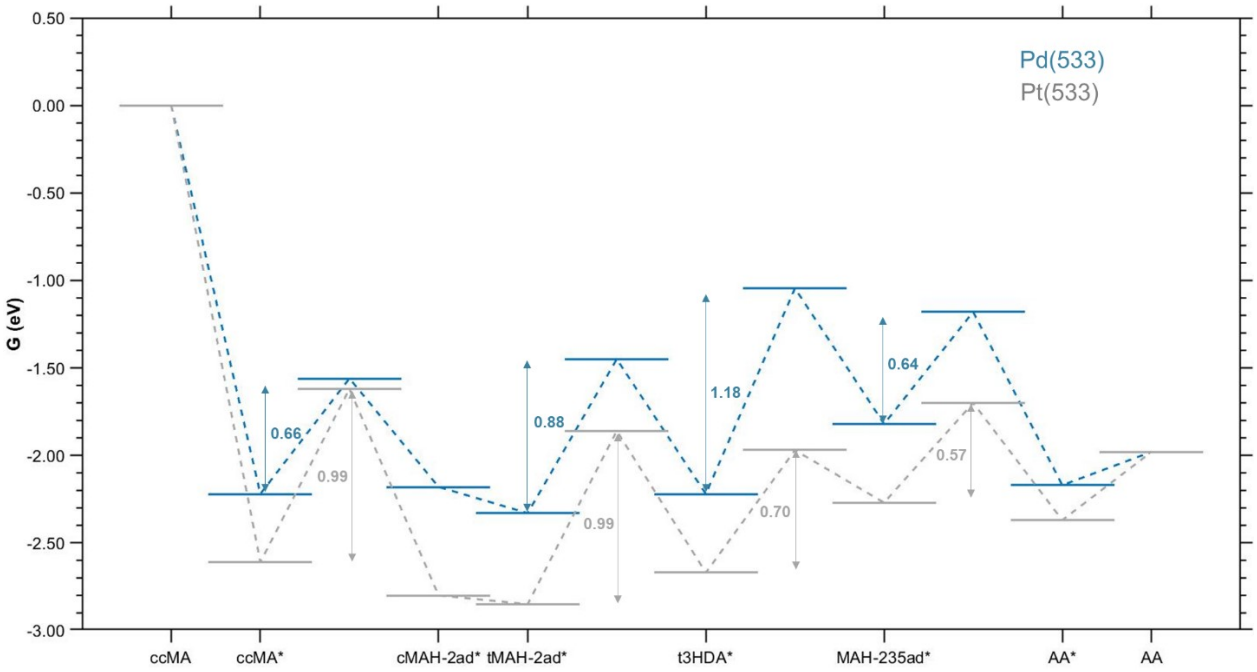

Fig. S9 Free energy (G, eV) diagram for *cc*MA* → *t*3HDA* → AA* pathway on Pd(533) and Pt(533) surfaces at 0.00 V_{RHE}, pH 0, and 298 K. Notation: *cis,cis*-muconic acid (*cc*MA), *trans*-3-hexenedioic acid (*t*3HDA), adipic acid (AA). Here, "*" denotes adsorbed species.

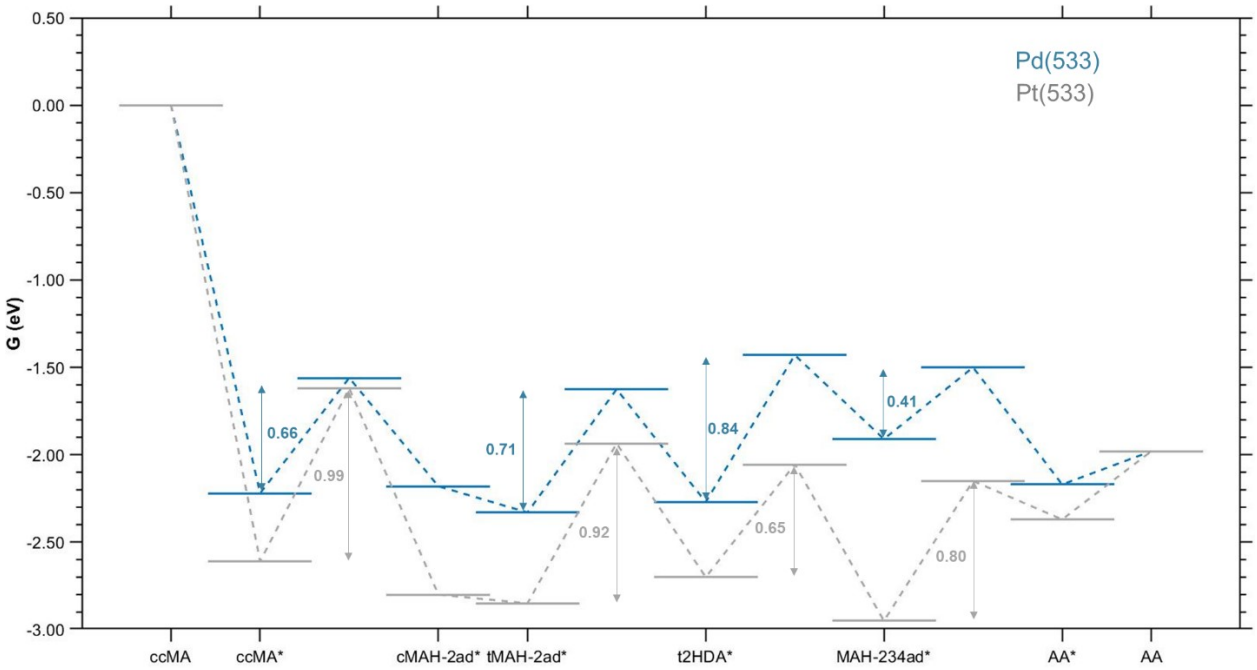

Fig. S10 Free energy (G, eV) diagram for *cc*MA* → *t*2HDA* → AA* pathway on Pd(533) and Pt(533) surfaces at 0.00 V_{RHE}, pH 0, and 298 K. Notation: *cis,cis*-muconic acid (*cc*MA), *trans*-2-hexenedioic acid (*t*2HDA), adipic acid (AA). Here, "*" denotes adsorbed species.

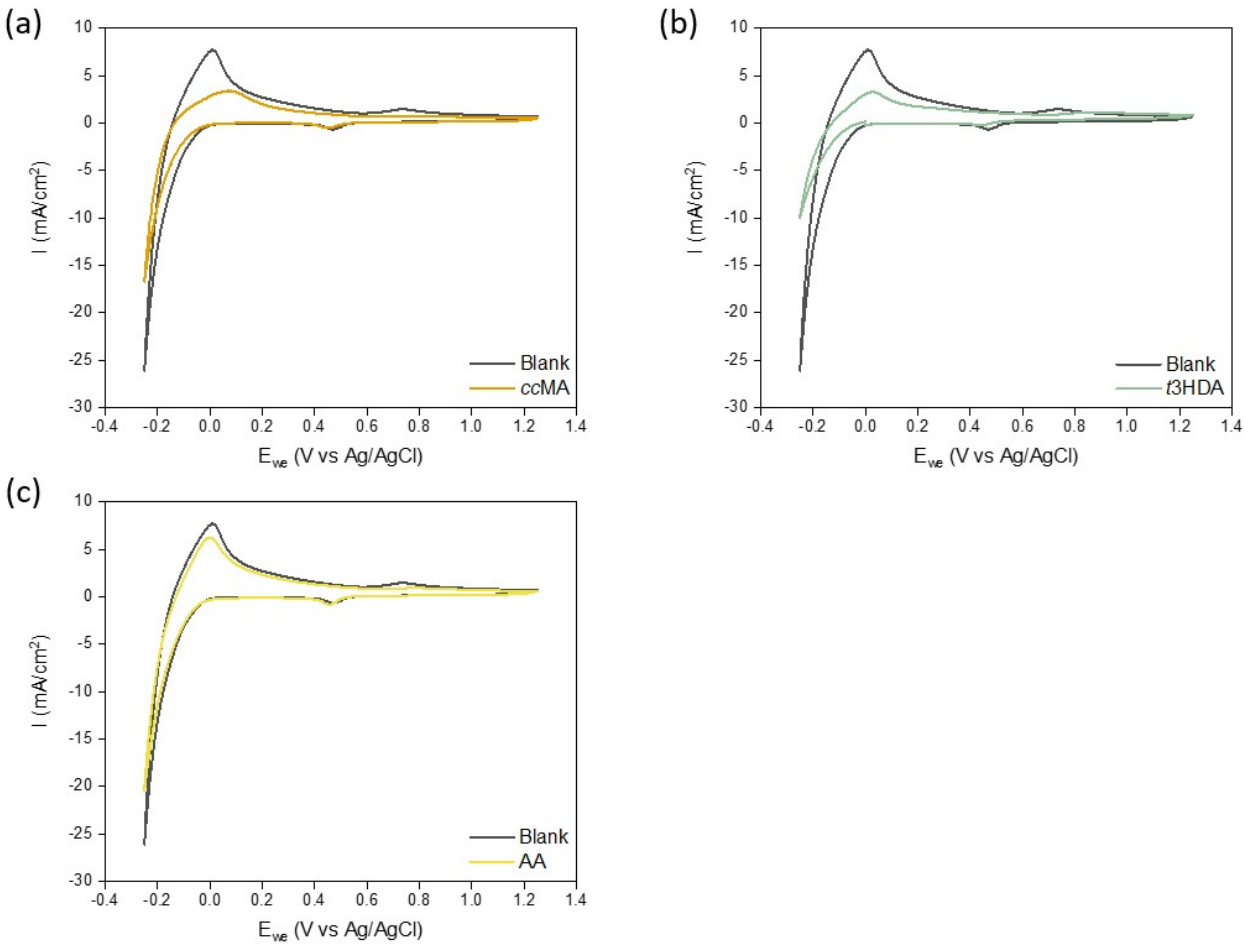

Fig. S11 Cyclic voltammograms for model solutions containing (a) *cc*MA, (b) *t*3HDA, and (c) AA, along with 0.1 M H_2SO_4 (blank) solution reference on polycrystalline Pd foil. Notation: *cis,cis*-muconic acid (*cc*MA), *trans*-3-hexenedioic acid (*t*3HDA), adipic acid (AA). Peak at ~ 0.6 $V_{Ag/AgCl}$ is characteristic for PdO_x reduction, and those in the range of 0.0 to -0.2 $V_{Ag/AgCl}$ are characteristic peaks for H* adsorption/desorption. The scan rate for obtaining CVs was set to 50 mV/sec.

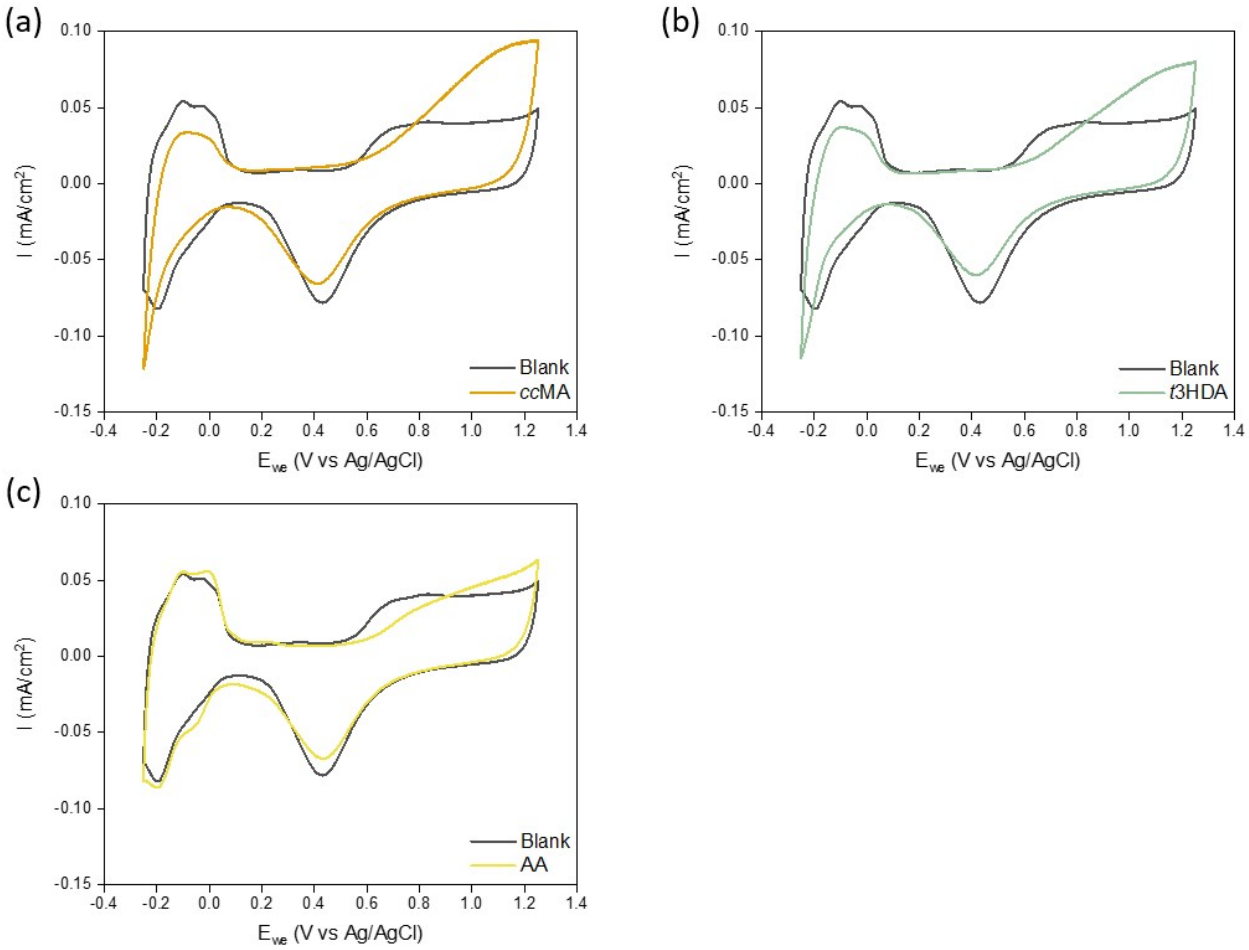

Fig. S12 Cyclic voltammograms for model solutions containing (a) *cc*MA, (b) *t*3HDA, and (c) AA, along with 0.1 M H_2SO_4 (blank) solution reference on Pt/C. Notation: *cis,cis*-muconic acid (*cc*MA), *trans*-3-hexenedioic acid (*t*3HDA), adipic acid (AA). Peak at ~ 0.4 $V_{Ag/AgCl}$ is characteristic for PtO_x reduction, and those in the range of 0.0 to -0.2 $V_{Ag/AgCl}$ are characteristic peaks for H* adsorption/desorption. The scan rate for obtaining CVs was set to 50 mV/sec.

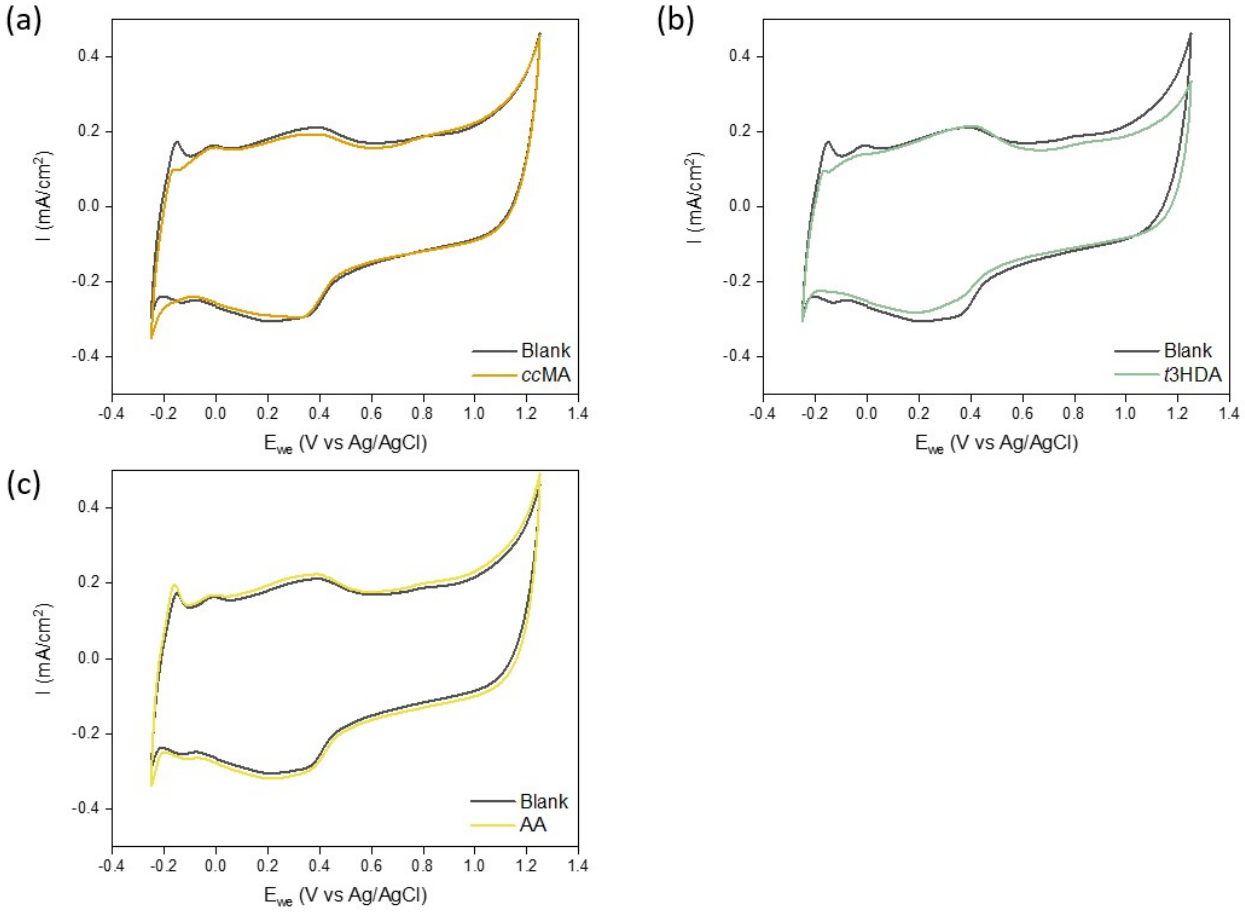

Fig. S13 Cyclic voltammograms for model solutions containing (a) *cc*MA, (b) *t*3HDA, and (c) AA, along with 0.1 M H_2SO_4 (blank) solution reference on Pd/C. Notation: *cis,cis*-muconic acid (*cc*MA), *trans*-3-hexenedioic acid (*t*3HDA), adipic acid (AA). Peak at ~ 0.4 $V_{Ag/AgCl}$ is characteristic for PdO_x reduction, and those in the range of 0.0 to -0.2 $V_{Ag/AgCl}$ are characteristic peaks for H* adsorption/desorption. The scan rate for obtaining CVs was set to 50 mV/sec.

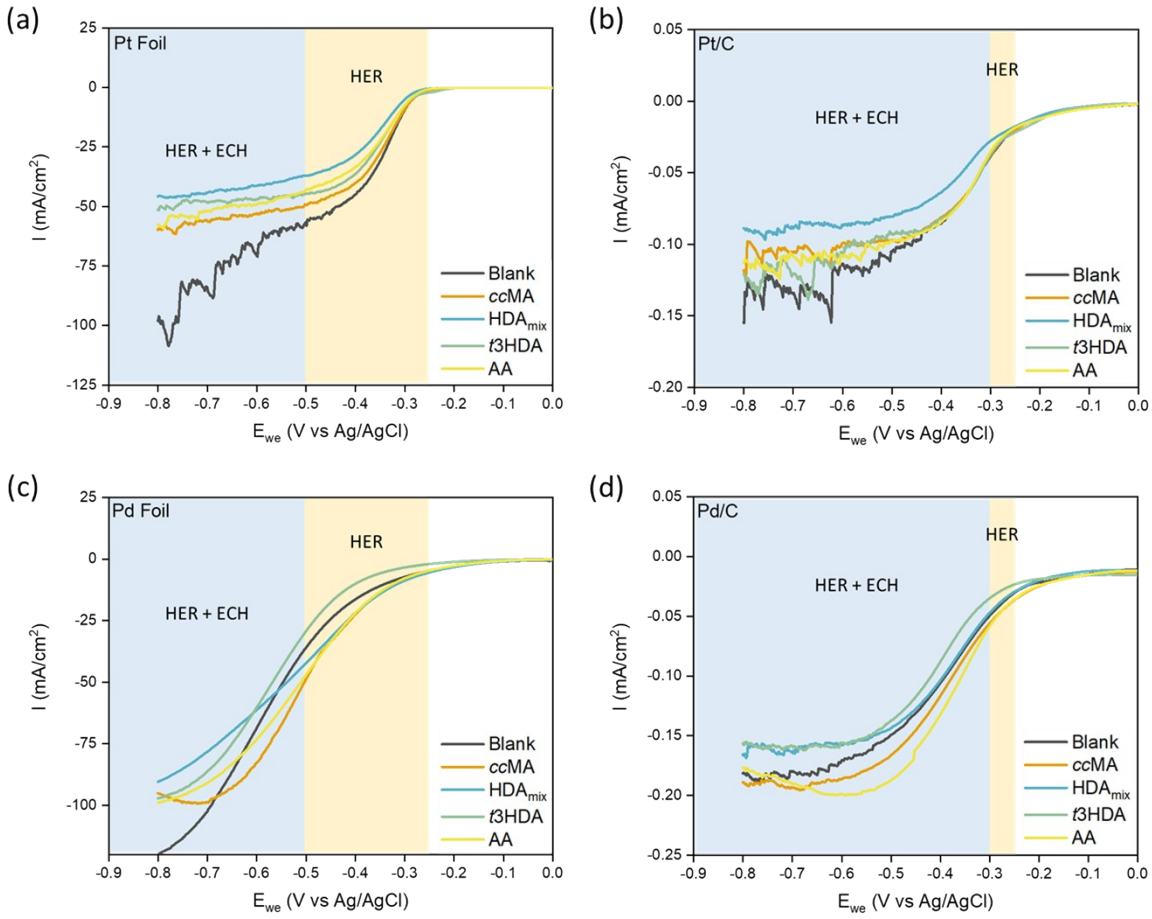

Fig. S14 Linear sweep voltammograms for respective model solutions on (a) Pt foil, (b) Pt/C, (c) Pd foil, and (d) Pd/C at pH 1. The sweep rate was set to 50 mV/sec. The regions in the LSVs are bifurcated based on chronoamperometry experiments in Fig. S1-S3, Fig. S7, and CVs in Fig. S8-S11. Notation: *cis,cis*-muconic acid (*cc*MA), *trans*-3-hexenedioic acid (*t*3HDA), adipic acid (AA).

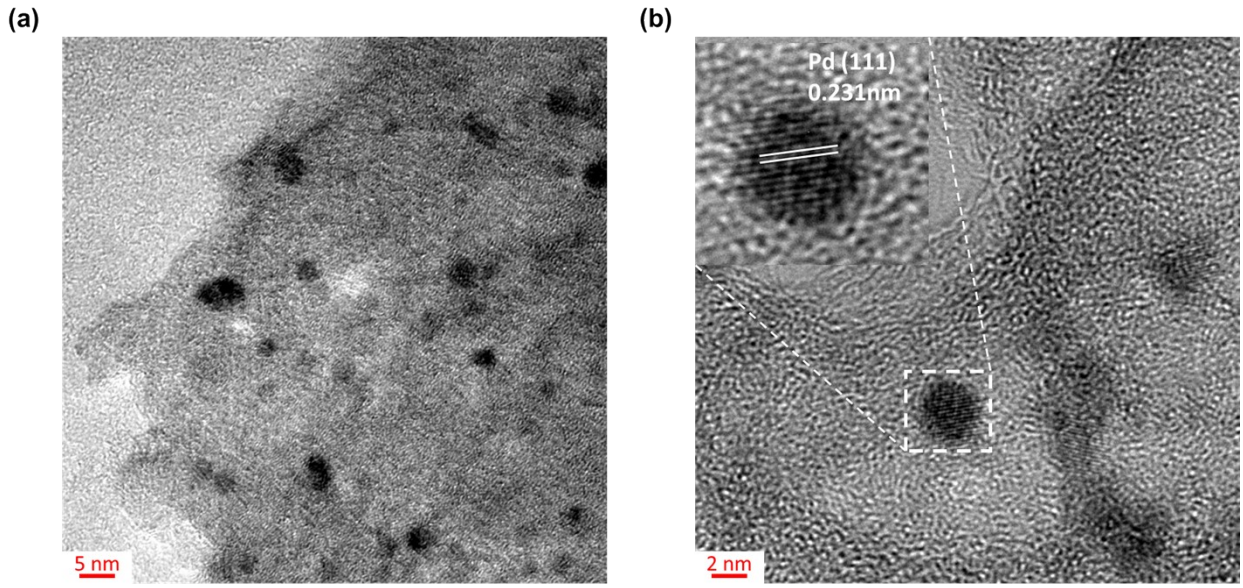

Fig. S15 High resolution transmission electron microscopy (HR-TEM) image of the fresh commercial 5 wt.% Pd/C catalyst (average particle size: 3 nm) at (a) 410 kx, and (b) 450 kx magnifications. The zoom-in inset image in (b) shows the d-spacing in the Pd lattice, which corresponds to the (111) facet of Pd.

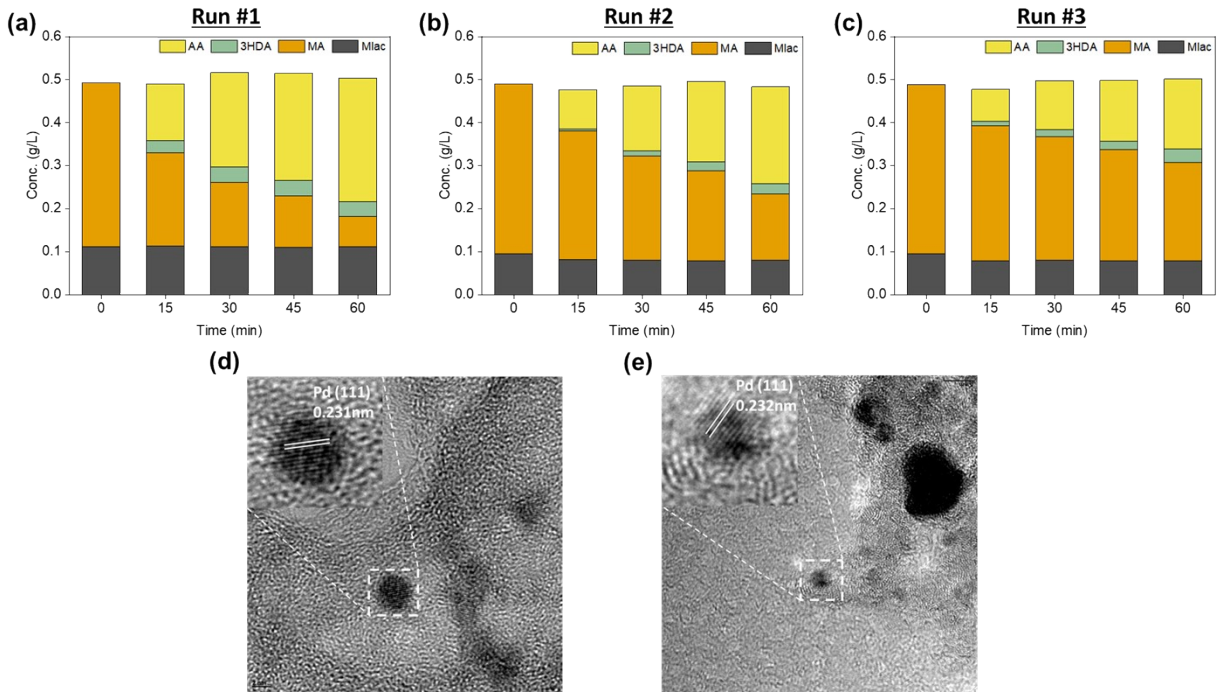

Fig. S16 (a)-(c) Concentration (g/L) of reactants and products vs. time (min) for three consecutive cycles of chronoamperometry (CA) experiments at -0.40 $V_{Ag/AgCl}$, pH 1 on Pd/C. (d) HR-TEM image of fresh Pd/C sample. (e) HR-TEM image of spent Pd/C sample.

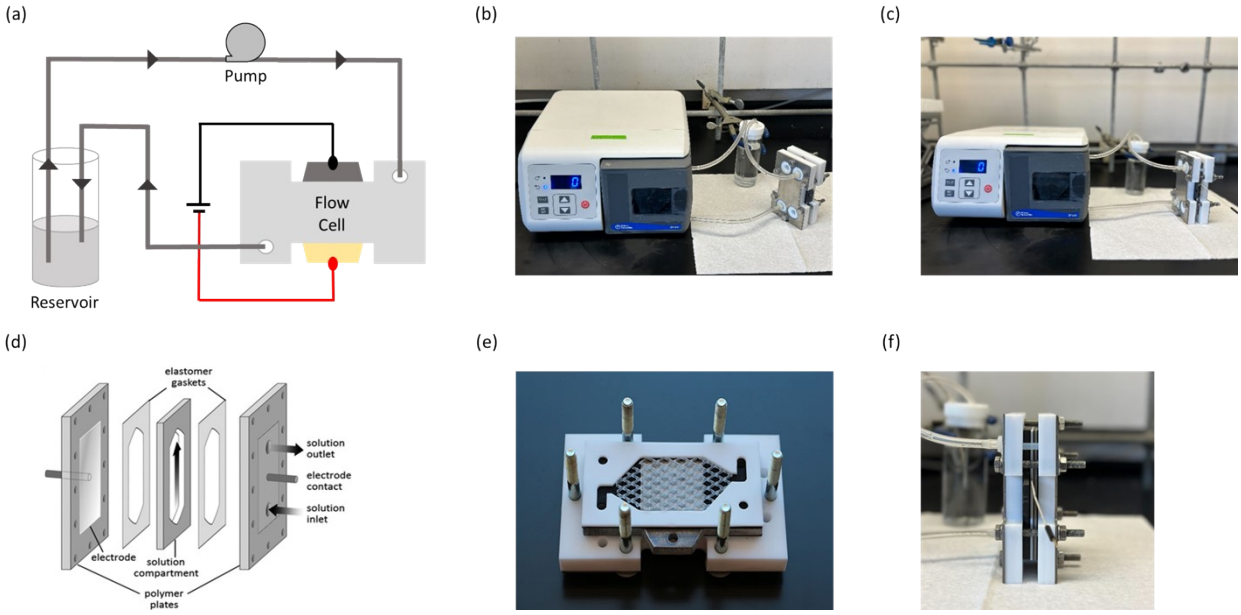

Fig. S17 (a) Schematic and (b)-(c) photographs of the experimental setup used in this study. (d) Schematic of the single-compartment electrochemical flow cell used in this study.[1] (e) Top view and (f) side view photographs of the single-compartment electrochemical flow cell.

Table S1. Calculated free energies (G_{A*}, eV) of reaction intermediates adsorbed on (111) and (533) surfaces of Pd and Pt at 298 K. All values are referenced to the clean surfaces, *cc*$MA_{(g)}$, and $H_{2(g)}$ at 298 K and 1 atm.

Chemical species	**Pd(111)**	**Pt(111)**	**Pd(533)**	**Pt(533)**
*cc*MA*	-1.91	-2.01	-2.22	-2.61
*c*MAH-2ad*	-1.61	-1.96	-2.19	-2.81
*t*MAH-2ad*	-1.70	-2.01	-2.34	-2.86
*c*MAH-3ad*	-1.41	-1.93	-2.03	-2.88
*t*MAH-3ad*	-1.50	-2.13	-2.17	-2.82
*c*MAH-23ad* (or *c*2HDA*)	-1.50	-1.91	-2.18	-2.36
*t*MAH-23ad* (or *t*2HDA*)	-1.61	-2.10	-2.28	-2.71
MAH-24ad*	-1.18	-2.15	-1.91	-2.59
*c*MAH-25ad* (or *c*3HDA*)	-1.45	-1.89	-2.16	-2.59
*t*MAH-25ad* (or *t*3HDA*)	-1.54	-2.07	-2.23	-2.68
MAH-34ad*	-1.35	-1.76	-1.98	-2.89
MAH-234ad*	-1.71	-2.00	-1.92	-2.96
MAH-235ad*	-1.50	-1.92	-1.83	-2.28
AA*	-2.18	-2.19	-2.18	-2.39
H*	-0.40	-0.32	-0.43	-0.58

Table S2. Calculated zero-point energies, entropies, and free energies of reaction intermediates in the solution phase at 298 K. Free energies are referenced to isolated *cc*MA and H_2 (ZPE: 0.27 eV, S: 130.3 J/(mol*K)) in implicit water at 298 K.

Chemical species	**ZPE (eV)**	**S (J/(mol*K))**	**G (eV)**
*cc*MA	3.14	416.6	0.00
*c*MAH-2ad	3.38	441.3	0.22
*c*MAH-3ad	3.38	451.6	0.72
*t*MAH-2ad	3.36	444.2	0.11
*t*MAH-23ad (or *t*2HDA)	3.73	439.3	-0.98
*t*MAH-25ad (or *t*3HDA)	3.71	444.4	-0.76
MAH-234ad	3.99	450.0	-0.18
MAH-235ad	3.96	464.9	0.02
AA	4.36	450.7	-1.80

Table S3. Calculated zero-point energies (ZPE_{A*}, eV) of reaction intermediates adsorbed on (111) and (533) surfaces of Pd at 298 K. The values on Pt surfaces were assumed to be the same as on Pd surfaces. ZPE_{A*} values on respective surfaces of Pt. ZPE for *cc*MA$_{(g)}$ is 3.07 eV, and $H_{2(g)}$ is 0.27 eV at 1 atm and 298 K.

Chemical species	**Pd(111)**	**Pd(533)**
*cc*MA*	3.05	3.08
*c*MAH-2ad*	3.35	3.37
*t*MAH-2ad*	3.35	3.36
*c*MAH-3ad*	3.35	3.40
*t*MAH-3ad*	3.35	3.37
*c*MAH-23ad* (or *c*2HDA*)	3.66	3.67
*t*MAH-23ad* (or *t*2HDA*)	3.65	3.65
MAH-24ad*	3.63	3.67
*c*MAH-25ad* (or *c*3HDA*)	3.65	3.64
*t*MAH-25ad* (or *t*3HDA*)	3.66	3.65
MAH-34ad*	3.61	3.71
MAH-234ad*	3.96	3.96
MAH-235ad*	3.96	3.97
AA*	4.27	4.24

Table S4. Calculated entropies (S_{A*}, J/(mol*K)) of reaction intermediates adsorbed on (111) and (533) surfaces of Pd at 298 K. The values on Pt surfaces were assumed to be the same as on Pd surfaces. Entropy for *cc*MA$_{(g)}$ is 428.2 J/(mol*K), and for $H_{2(g)}$ is 134.4 J/(mol*K) at 1 atm and 298 K.

Chemical species	**Pd(111)**	**Pd(533)**
*cc*MA*	195.8	187.6
*c*MAH-2ad*	208.8	203.2
*t*MAH-2ad*	183.8	196.7
*c*MAH-3ad*	190.4	185.6
*t*MAH-3ad*	203.9	199.7
*c*MAH-23ad* (or *c*2HDA*)	195.4	198.9
*t*MAH-23ad* (or *t*2HDA*)	191.9	201.0
MAH-24ad*	196.1	199.9
*c*MAH-25ad* (or *c*3HDA*)	215.7	207.7
*t*MAH-25ad* (or *t*3HDA*)	202.7	204.8
MAH-34ad*	197.2	193.3
MAH-234ad*	205.9	193.7
MAH-235ad*	236.3	196.2
AA*	241.6	228.4

Table S5. Calculated values of $U_{0,RHE}$ (eV) for potential dependent correction of activation free energies for various elementary steps involved in most favorable pathways on (111) and (533) surfaces of Pd and Pt. Here, "*" denotes adsorbed species.

Elementary	**Pd(111)**	**Pt(111)**	**Pd(533)**	**Pt(533)**
*cc*MA* + H* → *c*MAH-2ad*	-0.11	-0.51	0.12	0.41
*cc*MA* + H* → *c*MAH-3ad*	0.07	-0.03	0.29	0.30
*t*MAH-2ad* + H* → *t*MAH-23ad*	0.46	-0.22	0.35	0.17
*t*MAH-2ad* + H* → *t*MAH-25ad*	0.09	0.22	0.42	0.20
*t*MAH-23ad* + H* → MAH-234ad*	-0.02	-0.60	0.06	0.29
*t*MAH-25ad* + H* → MAH-235ad*	0.17	-0.59	-0.03	0.30
MAH-234ad* + H* → AA*	0.21	0.15	0.58	0.02
MAH-235ad* + H* → AA*	-0.07	-0.25	0.32	0.26

Table S6. Calculated activation free energies ($G_a(U_{0,RHE})$, eV) for various elementary steps involved in most favorable pathways on (111) and (533) surfaces of Pd and Pt without any potential dependent corrections. Here "*" denotes adsorbed species.

Elementary	**Pd(111)**	**Pt(111)**	**Pd(533)**	**Pt(533)**
*cc*MA* + H* → *c*MAH-2ad*	0.83	0.22	0.72	1.04
*cc*MA* + H* → *c*MAH-3ad*	1.17	0.74	1.32	1.38
*t*MAH-2ad* + H* → *t*MAH-23ad*	0.87	0.76	0.73	0.95
*t*MAH-2ad* + H* → *t*MAH-25ad*	0.69	1.03	0.94	1.04
*t*MAH-23ad* + H* → MAH-234ad*	0.45	0.25	0.87	0.79
*t*MAH-25ad* + H* → MAH-235ad*	0.92	0.94	1.16	0.85
MAH-234ad* + H* → AA*	0.92	0.86	0.70	0.81
MAH-235ad* + H* → AA*	0.51	0.87	0.80	0.70

References

1 D. Pletcher, R. A. Green and R. C. D. Brown, *Chem. Rev.*, 2018, **118**, 4573–4591.